Differential microscopy for fluorescence-detected nonlinear absorption linear anisotropy based on a staggered two-beam femtosecond Yb:KGW oscillator

Daaf Sandkuijl,[1,*] Richard Cisek,[1] Arkady Major,[2] and Virginijus Barzda[1]

[1]*Department of Chemical and Physical Sciences, Department of Physics and Institute for Optical Sciences, University of Toronto, 3359 Mississauga Rd. North, Mississauga, ON, L5L 1C6, Canada*
[2]*Department of Electrical and Computer Engineering, University of Manitoba, 75 Chancellor's Circle, Winnipeg, MB, R3T 5V6, Canada*
**d.sandkuijl@utoronto.ca*

Abstract: We present a new laser system and nonlinear microscope, designed for differential nonlinear microscopy. The microscope features time-correlated single photon counting of multiphoton fluorescence generated by an alternating pulse-train of orthogonally polarized pulses. The generated nonlinear signal is separated using home-built electronics. Results are presented on fluorescence-detected nonlinear absorption linear anisotropy (FDNALA) of chloroplasts in *Asparagus Sprengerii Regel* and of Congo Red-stained cellulose.

OCIS codes: (180.4315) Nonlinear microscopy; (140.3615) Lasers, Ytterbium.

References and links

1. R. Carriles, K. E. Sheetz, E. E. Hoover, J. A. Squier, and V. Barzda, "Simultaneous multifocal, multiphoton, photon counting microscopy," Opt. Express **16**(14), 10364–10371 (2008).
2. R. Cisek, L. Spencer, N. Prent, D. Zigmantas, G. S. Espie, and V. Barzda, "Optical microscopy in photosynthesis," Photosynth. Res. **102**(2-3), 111–141 (2009).
3. I.-H. Chen, S.-W. Chu, C.-K. Sun, P.-C. Cheng, and B.-L. Lin, "Wavelength dependent damage in biological multi-photon confocal microscopy: A micro-spectroscopic comparison between femtosecond Ti:sapphire and Cr:forsterite laser sources," Opt. Quantum Electron. **34**(12), 1251–1266 (2002).
4. A. Major, R. Cisek, and V. Barzda, "Femtosecond Yb:KGd(WO_4)($_2$) laser oscillator pumped by a high power fiber-coupled diode laser module," Opt. Express **14**(25), 12163–12168 (2006).
5. A. Major, V. Barzda, P. A. E. Piunno, S. Musikhin, and U. J. Krull, "An extended cavity diode-pumped femtosecond Yb:KGW laser for applications in optical DNA sensor technology based on fluorescence lifetime measurements," Opt. Express **14**(12), 5285–5294 (2006).
6. U. Keller, K. J. Weingarten, F. X. Kartner, D. Kopf, B. Braun, I. D. Jung, R. Fluck, C. Honninger, N. Matuschek, and J. Aus der Au,, "Semiconductor saturable absorber mirrors (SESAM's) for femtosecond to nanosecond pulse generation in solid-state lasers," IEEE J. Sel. Top. Quantum Electron. **2**(3), 435–453 (1996).
7. G. R. Holtom, "Mode-locked Yb:KGW laser longitudinally pumped by polarization-coupled diode bars," Opt. Lett. **31**(18), 2719–2721 (2006).
8. G. Steinbach, I. Pomozi, O. Zsiros, A. Pay, G. V. Horvath, and G. Garab, "Imaging fluorescence detected linear dichroism of plant cell walls in laser scanning confocal microscopy," Cytometry A **73A**(3), 202–208 (2008).
9. L. Finzi, C. Bustamante, G. Garab, and C.-B. Juang, "Direct observation of large chiral domains in chloroplast thylakoid membranes by differential polarization microscopy," Proc. Natl. Acad. Sci. U.S.A. **86**(22), 8748–8752 (1989).
10. P. J. Walla, J. Yom, B. P. Krueger, and G. R. Fleming, "Two-photon excitation spectrum of light-harvesting complex II and fluorescence upconversion after one- and two-photon excitation of the carotenoids," J. Phys. Chem. B **104**(19), 4799–4806 (2000).
11. H. Puchtler, F. Sweat, and M. Levine, "On the binding of Congo red by amyloid," J. Hist. Cyt **10**(3), 355–364 (1962).
12. R. M. Brown, Jr., A. C. Millard, and P. J. Campagnola, "Macromolecular structure of cellulose studied by second-harmonic generation imaging microscopy," Opt. Lett. **28**(22), 2207–2209 (2003).

#133909 - $15.00 USD Received 23 Aug 2010; revised 9 Sep 2010; accepted 10 Sep 2010; published 14 Sep 2010

1. Introduction

Differential nonlinear microscopy is a new technique for simultaneously measuring the difference in signal between two imaging conditions. The technique was introduced recently and so far work has been done on differential polarization microscopy of second harmonic generation, and differential microscopy using beams with different focal depths [1].

Differential microscopy is especially useful in the imaging of highly dynamic biological samples, due to its immunity to dynamics on a timescale longer than the inter-pulse spacing. Since in a typical mode-locked laser oscillator the delay between two consecutive pulses is on the order of 10 ns this means that e.g. photobleaching, movement of the sample, or slow photo-adaptation do not distort the difference between two measured signals. Normally, sequential imaging of dynamic samples with different excitation conditions can make quantitative comparison nearly impossible unless large amounts of identical measurements are performed or the sample is completely static.

The differential microscopy technique relies on combining two synchronized pulsed laser beams such that in the time domain the pulses of one beam fall in between the pulses of the other beam. An electric reference pulse signal from one of the beams is then used to electronically sort every signal photon into the appropriate channel [1].

Since the routing works for any two synchronized laser beams, the beams can differ in any way; i.e. they can have different polarizations, wavelengths, intensities or other properties. This makes the technique highly versatile and applicable in most situations where a measurement is meant to determine the difference between two excitation conditions.

In this article we first present a laser system optimized for differential nonlinear microscopy. The laser is based on an Yb:$KGd(WO_4)_2$ (Yb:KGW) crystal and radiates around 1028 nm. This wavelength is highly useful for nonlinear microscopy in general due to the low absorption in biological materials [2,3]. In addition, the laser cavity is designed with output couplers on opposite ends of the cavity. This creates and intrinsic time-stagger of the pulses from the output beams, so that an external delay line is not necessary.

Next we present a nonlinear microscope with home-built routing electronics for differential microscopy and, as a proof of concept, the results we obtained for fluorescence-detected nonlinear absorption linear anisotropy (FDNALA) in chloroplasts from *Asparagus Sprengerii Regel* and in Congo red-stained corn stalk.

2. Laser and microscope setup

2.1 Laser design and specifications

The schematic of the laser cavity setup is shown in Fig. 1(a) and is based on our previously developed high-power continuous wave and mode-locked oscillators [4]. As a pump source, we used a 25 W fiber coupled laser diode operating at 980 nm (Apollo Instruments). The diameter of the fiber was 200 µm with a numerical aperture (NA) of 0.22.

The pump radiation was focused into a 3 mm long anti-reflection coated plane/plane Yb:KGW crystal with 5% Yb-doping (EKSMA Optics) through a dichroic mirror DM1 using two spherical lenses. The spot size of the pump was determined to be about 250 µm. The dichroic mirror DM1 was coated for high transmission (>95%) at the pump wavelength and high reflection (>99.9%) in the 1020-1080 nm region. The rest of the cavity mirrors were coated for high reflection (>99.9%) in the 1020-1080 nm region, unless specified otherwise. All mirrors were custom designed by Laseroptik GmbH. The angles between the cavity mode and the normals of the mirrors were kept to a minimum to minimize astigmatism, but half-angles of 3.7°, 2.5° and 1.6° were necessary for dichroic mirror DM1 and curved mirrors M1 and M2, respectively [4]. The crystal was sandwiched between two thermo-electric elements and cooled down to 10 °C.

Curved cavity mirrors M1 and M2 had radii of curvature of 500 mm and ensured a good overlap of the lasing mode with the pump mode. The cavity length was extended by 8 meters using two identical telescopes (omitted from the figure for clarity) with an imaging ratio of 1:1, similar to our previous design [5]. As a result, the cavity repetition rate was reduced to

#133909 - $15.00 USD Received 23 Aug 2010; revised 9 Sep 2010; accepted 10 Sep 2010; published 14 Sep 2010

14.3 MHz and the temporal separation between two consecutive pulses increased to about 70 ns. The laser design is highly suitable for multiplexed fluorescence excitation, since the beams are coupled from opposite ends of the cavity and thus have alternating pulses with approximately 35 ns spacing.

One of the cavity arms was terminated by a semiconductor saturable absorber mirror (SESAM, SAM-1040-2-25.4s-500fs, BATOP GmbH) [6], which initiated and sustained the mode locking process. To exploit soliton shaping effects during femtosecond pulse formation we used two dispersive mirrors inside the cavity (GTI, Layertec GmbH). Both mirrors introduced −1200 fs^2 of dispersion per reflection and were mainly used to compensate for the positive dispersion and self-phase modulation in the laser crystal. For the experiments, a total of approximately 18% output coupling (output couplers OC1 and OC2) was used.

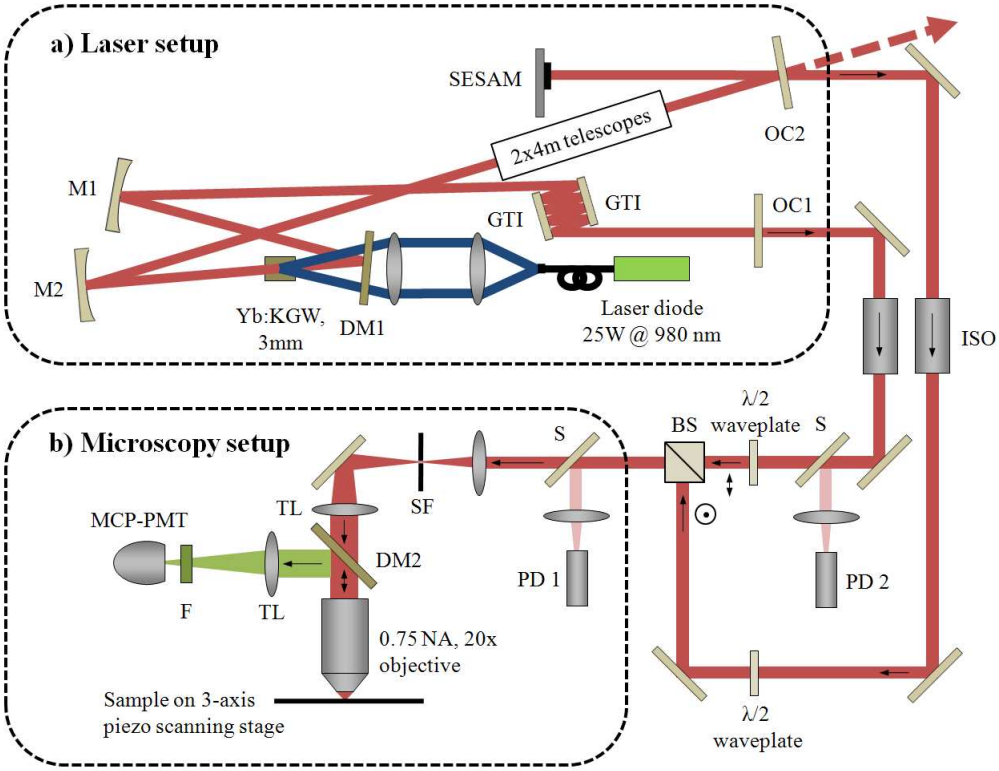

Fig. 1. Schematic of the laser cavity (a) and microscope setup (b). M1, M2 – curved mirrors; SESAM – saturable absorber mirror; OC – output coupler; GTI – Gires-Tournois dispersion compensation mirrors; ISO – optical isolator; DM – dichroic mirror; S – 4% reflection glass sampler; F – RG665 and 3x SP750 filters; BS – polarizing cube beamsplitter; SF – spatial filter; MCP-PMT – microchannel plate photomultiplier tube; PD 1 – photodiode for stop signal; PD 2 – photodiode for routing signal; TL – tube lens.

At incident pump power of 20.5W onto the crystal (~75% absorbed by the crystal), we generated up to 3.1W of average output power in a stable train of ~430 fs soliton-like pulses. At a repetition rate of 14.3 MHz this corresponded to 217 nJ of pulse energy or a peak power of 505 kW. It should be noted that a recent demonstration of similar pulse energies from a Yb:KGW laser required a pump power more than twice as high [7]. Single pulse operation was achieved for −19200 fs^2 of introduced negative dispersion. The mode-locking process was stable and did not have any tendencies towards Q-switching instabilities.

An estimate of the pulse duration was obtained with a second order autocorrelator based on two-photon absorption in a red light-emitting diode, yielding a pulse duration of 430 fs, assuming a *sech*^{2} temporal profile in the analysis. The spectral width of the pulses was

#133909 - $15.00 USD Received 23 Aug 2010; revised 9 Sep 2010; accepted 10 Sep 2010; published 14 Sep 2010

measured to be 3.0 nm. From this, the time-bandwidth product for the pulses was calculated to be 0.36, indicating that the pulses were nearly transform-limited. It should be noted that the autocorrelation measurement took place after passing the pulses through an optical isolator and about 4 meters of air.

Passive mode locking was not completely self-starting and required a very light tap on the optical table. Once initiated, mode locking could be sustained for hours of operation despite quite strong ambient air currents. The mode spot diameter on the SESAM was calculated to be ~350 μm and corresponded to a maximum energy fluence of 1.5 mJ/cm^2. No damage to the SESAM was observed during the experiments. Occasionally, depending on cavity alignment, pulse splitting was observed.

2.2 Microscope setup

The laser beams were passed through half-wave plates and combined using a polarizing cube beamsplitter (Union Optics). The polarizing cube had contrast ratio of more than 1000:1 between horizontal and vertical polarization. As a result, the half-wave plates controlled the intensity of the light that was passed through the polarizing cube from the beams, while the beamsplitter ensured that the combined beam consisted of orthogonally polarized pulses from the beams. A photodiode (PD 2, Becker & Hickl GmbH) generated a reference pulse-train from one of the Yb:KGW beams. The signal from this photodiode was fed into a discriminator which generated a TTL signal with approximately 35 ns uptime. The TTL signal was fed into home-built routing electronics, which were connected to the routing input of the single photon counting card (SPC-830, Becker & Hickl GmbH).

Since the beams originate from output couplers at opposite ends of the cavity, the combined beam consists of a pulse-train alternating between vertically and horizontally polarized pulses with approximately 35 ns spacing between them. The cavity design therefore precludes the need for a long delay line on the optical table. A second photodiode (PD 1, Becker & Hickl GmbH) generated a reference pulse-train from the combined beam which was used as the stop-signal for the synchronization of the time-correlated single photon counting (TCSPC).

The excitation and signal collection was provided by a 20x 0.75 NA air objective (Zeiss). Both polarized beams completely filled the back aperture of the objective. A dichroic mirror (DM2, HR: 565-720 nm, HT: 790-1500 nm, R&G Co.) reflected the fluorescence signal, which was passed through a tube lens (TL, Zeiss), focusing the fluorescence signal into the detector. A filter set (F, RG665, CVI Melles Griot and 3x SP750, Thorlabs) separated the fluorescence signal from the Yb:KGW beam. A microchannel plate photomultiplier tube (MCP-PMT, Hamamatsu R3809U-50) was used to detect the fluorescence photons. The FWHM of the instrument response of the detector was about 60 ps (data not shown).

Sample scanning was done by an XYZ piezoelectric stage (Physik Instrumente GmbH) synchronized with the detection electronics. The pixel dwell time was approximately 0.8 ms.

In all of the following work, the input beam powers were normalized by equalizing the the two-photon excitation fluorescence signal by each beam from a 16 μM Rhodamine B solution.

2.3 Chloroplast sample preparation

Measurements were done on single cells from *Asparagus Sprengerii Regel*, an ornamental type of asparagus. Due to limited binding between cells in the leaves of the plant, single cells could easily be separated and imaged. To ensure the chloroplasts did not move during the experiments, the cells were fixed in a 5% poly-acrylamide gel before imaging. The cells were isolated and embedded in gel under low-light conditions and imaged with a pulse energy of 0.2 nJ.

2.4 Staining cellulose with Congo Red

Previous work has shown that Congo Red binds to cellulose in a structured manner, leading to anisotropy in the fluorescence excitation of cellulose-bound Congo Red [8]. In the current work, dried corn stalk was stained with Congo Red in a 0.3 mM solution for 10 minutes and

#133909 - $15.00 USD Received 23 Aug 2010; revised 9 Sep 2010; accepted 10 Sep 2010; published 14 Sep 2010

subsequently washed for 15 minutes with a 1M NaCl solution. A thin slice of the stained corn stalk was then imaged in the microscope described above with a pulse energy of approximately 2 nJ.

3. Results

3.1 Multiplexed absorption anisotropy imaging of chloroplasts

Figure 2 shows results obtained from the measurements on the *Asparagus* sample. The plant cells consist of a large central vacuole surrounded by chloroplasts, which are roughly disc-shaped organelles arranged along the cell wall. The chloroplasts contain grana with stacked photosynthetic membranes oriented predominantly along the plane of the disc [9].

The nonlinear absorption in the sample for light at 1028 nm is dominated by carotenoids in pigment protein complexes [10]. The fluorescence was collected in the wavelength range of 665 - 750 nm, corresponding to chlorophyll fluorescence [10]. If nonlinear absorption anisotropy is present in the sample, it is expected to show up as a difference in absorption of light polarized parallel or perpendicular to the membranes in the chloroplasts.

Figures 2(a) and 2(b) represent the fluorescence intensity obtained for each channel, from which it is clear that there is significant FDNALA in the sample. Figure 2(c) quantifies this anisotropy as $(I_1\text{-}I_2)/(I_1 + I_2)_{max}$, which has a theoretically possible range from −1 to + 1. The anisotropy is most prevalent when the chloroplast is imaged with the light propagation direction along the grana membranes, and the membranes oriented along one of the incident polarizations. This can be seen clearly, for instance, in the chloroplasts labeled *1* and *2*. Interestingly, the chloroplast labeled *3* shows both orientations of photosynthetic membranes due to the curved organization of the grana along the inward-facing envelope membrane. The anisotropy can be seen to change sign inside this chloroplast in Fig. 2(c). The chloroplast labeled *4* is face-aligned, which implies the grana membranes are most probably perpendicular to the propagation direction of the light. The orientation distribution of pigment-protein complexes within the photosynthetic membranes is very large, leading to low anisotropy in face-aligned chloroplasts.

While the microscope is able to provide time-resolved information about the photon counts for each pixel, no significant conclusions about differences in lifetimes for the two polarizations could be drawn from the data.

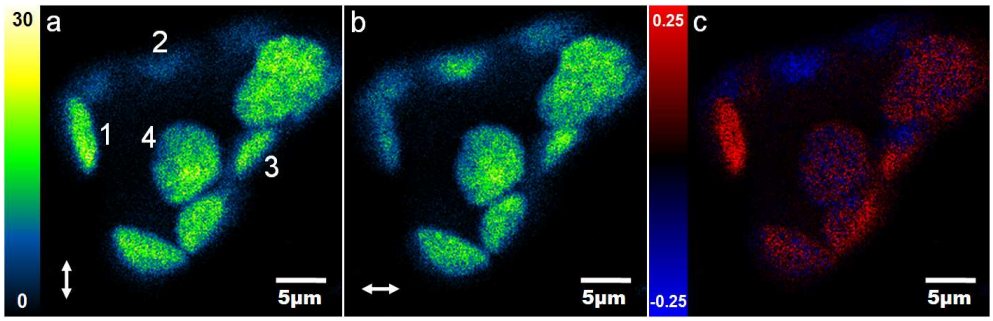

Fig. 2. Fluorescence measurements from chloroplasts in a single cell of *Asparagus Sprengerii Regel*. (a,b) Fluorescence intensity images, obtained simultaneously. The arrows indicate the polarization direction. Chloroplasts were labeled 1 through 4 for comparison purposes in the text. (c) FDNALA of the fluorescence signal, defined as $(I_1\text{-}I_2)/(I_1 + I_2)_{max}$.

3.2 Multiplexed absorption anisotropy imaging of Congo Red stained cellulose

Figure 3 shows the results obtained from the Congo Red-stained sample. The FDNALA is maximal when the polarization of one of the beams is parallel to the cellulose fiber orientation. This is in line with the commonly accepted hypothesis of Congo Red binding to cellulose fibers [11], namely that the diphenol backbone of Congo Red is lined up with the fiber direction, assuming that the nonlinear fluorescence excitation cross-section is maximal

#133909 - $15.00 USD Received 23 Aug 2010; revised 9 Sep 2010; accepted 10 Sep 2010; published 14 Sep 2010

for light polarized along the diphenol backbone of the Congo Red molecule. Since the sample consisted mostly of water and cellulose and the scanning depth was between 50 and 100 µm, depolarization of the beams was not observed [8]. However, deeper imaging in highly depolarizing media might deteriorate the FDNALA signal.

Second harmonic signal is also generated by cellulose at the imaging intensities we used, and by changing the detection filters, or adding a detector, our setup can be used to obtain similar anisotropy images for second harmonic generation from cellulose [1,12].

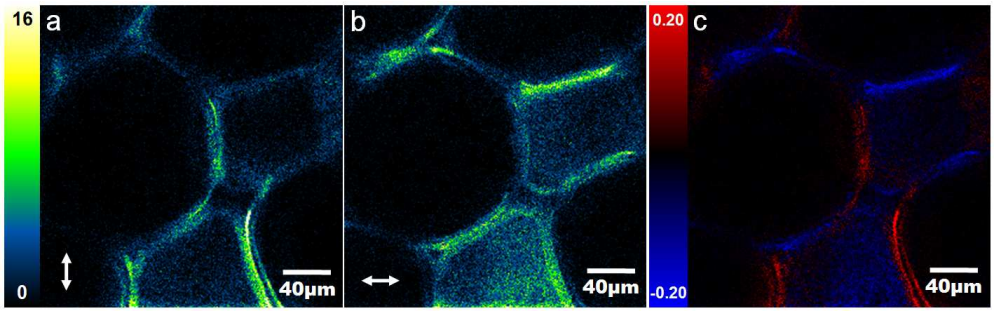

Fig. 3. Fluorescence intensity from Congo Red stained corn stalk. (a,b) Fluorescence intensity images, obtained simultaneously. The arrows indicate the polarization direction. (c) FDNALA of the signal, defined as $(I_1-I_2)/(I_1 + I_2)_{max}$. Maximum FDNALA occurs when the polarization is lined up with the cellulose fibers in the corn stalk.

5. Conclusion and outlook

The technique of differential nonlinear microscopy was demonstrated by multiplexed imaging of several samples with electronically separated detection using a home-built femtosecond Yb:$KGd(WO_4)_2$ laser. The microscope is able to simultaneously image with two different polarization orientations by using an alternating pulse-train of orthogonally polarized pulses. As a result, the nonlinear absorption linear anisotropy of a sample can be determined in a single measurement.

Similar linear techniques are also available, but they lack the temporal resolution offered by alternating pulse-trains and require confocal microscopy setups, which suffer from out-of-focus photobleaching. However, since the transition dipole moment can be different for linear and nonlinear excitation, the techniques can complement each other and provide more information about the molecular properties at the focus.

The measurements of fluorescence-detected nonlinear absorption linear anisotropy (FDNALA) in chloroplasts showed that the nonlinear absorption of light is strongest for light polarized parallel to the grana membrane plane. Since the carotenoids in photosynthetic antenna pigment-protein complexes are mostly responsible for the nonlinear absorption of light around 1028 nm, the nonlinear excitation dipole moment of these carotenoids is expected to be oriented close to the membrane plane.

The measurements on Congo Red-stained corn stalk (cellulose) are consistent with the commonly accepted hypothesis that Congo Red binds to cellulose with its diphenol backbone oriented along the fiber direction, which makes for higher nonlinear absorption when the light is polarized along the fiber.

Since the separation electronics are insensitive to the difference between the pulses, it is possible to vary any other parameter of the excitation light between the beams and still separate the generated signal. Therefore, differential polarization measurements are only one example of the application of this technique.

Acknowledgements

D.S. was supported by the Carolus Magnus Fund and the Pieter Beijer Fund through a Prince Bernhard Culture Fund scholarship. The authors acknowledge support from the Natural Sciences and Engineering Research Council of Canada, the Ontario Innovation Trust, the

Ontario Centre of Excellence for Photonics, the Canada Foundation for Innovation and the University of Manitoba.

#133909 - $15.00 USD Received 23 Aug 2010; revised 9 Sep 2010; accepted 10 Sep 2010; published 14 Sep 2010